Solar forcing as an important trigger for West Greenland sea-ice variability over the last millennium

Supplementary material

Longbin Sha, Hui Jiang, Marit-Solveig Seidenkrantz, Raimund Muscheler, Xu Zhang, Mads Faurschou Knudsen, Jesper Olsen, Karen Luise Knudsen, Weiguo Zhang

Correspondence and requests for materials should be sent to L. Sha (shalongbin@hotmail.com)

Table of contents

1. Chronology

The chronology for gravity core GA306-GC4 was constructed on the basis of 10 AMS ^{14}C ages. Box core GA306-BC4, retrieved at the same location as gravity core GA306-GC4, was analysed for the activity of ^{210}Pb, ^{226}Ra and ^{137}Cs via gamma spectrometry at the Gamma Dating Centre, Department of Geosciences and Natural Resource Management, University of Copenhagen, Denmark (Sha et al., 2012; Erbs-Hansen et al., 2013). An age-depth model for GA306-BC4 was obtained by applying a modified CRS-modelling approach (Appleby, 2001; Sha et al., 2012) combined with one AMS ^{14}C age determination. There is an age overlap of 5 years between the age model for GA306-BC4 and that for GA306-GC4 (Erbs-Hansen et al., 2013) (see Figure S1).

Table S1. AMS ^{14}C age determinations for core sites GA306-GC4 and GA306-BC4. The ^{14}C ages were calibrated with OxCal 4.1 software (Ramsey, 2009) using the Marine09 calibration dataset (Reimer et al., 2009) with a ΔR of 140±30 years (Erbs-Hansen et al., 2013). The modelled age is at a 95.4% confidence interval. The agreement index between model and sample is given in brackets. Modelled ages marked with "n/a" were not used in the age model.

Laboratory code	Material (Mollusc shell)	Original depth (cm)	Corrected depth (cm)	$\delta^{13}C$ (‰)	$\delta^{18}O$ (‰)	Age (^{14}C yr BP)	Modelled age (cal. yr BP)
GA306-BC4							
AAR-11685	*Thyasira gouldi*	26–27	26.5	-4.42	2.35	490±25	n/a
AAR-11684	*Thyasira gouldi*	39–40	39.5	-2.31	1.72	638±27	34–17 (78.4%)
GA306-GC4							
AAR-11694	*Thyasira gouldi*	8–9	41.2	-3.62	1.44	531±27	40–20 (139.7%)
AAR-14536	*Yoldia hyperborea*	50–51	83.2	-0.52	4.09	642±22	86–52 (89.1%)
AAR-11693	*Thyasira gouldi*	141–142	174.2	-3.57	1.96	706±42	132–89 (128.3%)
AAR-11692	*Thyasira gouldi*	151–153	184.7	-4.01	2.02	826±30	315–257 (51.1%)
AAR-11691	*Thyasira gouldi*	241–243	274.7	-2.33	2.03	984±31	337–279 (124.9%)
AAR-11690	*Thyasira gouldi*	291–292	324.2	-5.76	0.73	1095±33	525–455 (117.3%)
AAR-11689	*Megayoldia thraciaeformis*	345–346	378.2	0.31	2.25	1230±37	630–555 (88.8%)
AAR-11688	*Nuculana pernula costigera*	383–385	416.7	0.38	2.08	1434±35	749–657 (57.1%)
AAR-11687	*Macoma moesta*	426–427	459.2	0.21	2.45	1497±33	836–736 (95.9%)
AAR-11686	*Thyasira gouldi*	452–453	485.2	-2.71	2.15	1516±32	931–821 (114.1%)

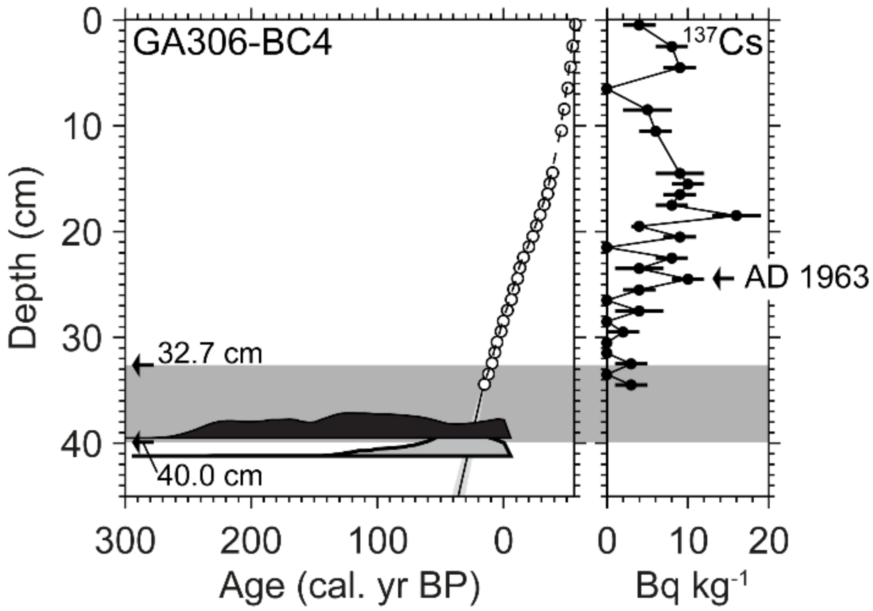

Figure S1. Age-depth model for box core GA306-BC4. The left panel shows the ^{210}Pb CRS model together with the ^{14}C-based age model, along with the ^{14}C chronological information. The horizontal grey shaded area indicates the overlap between the box and gravity cores.

2. Surface sediment samples

In total, 72 surface sediment samples were used in the modern calibration dataset. The locations and water depths of these surface samples are listed in Table S2.

Table S2. Location and water depth (m) of the surface samples. Samples marked with "+" were provided by Anne Jennings, INSTAAR, University of Colorado in Boulder, USA; and sample JM96-1219/1 was provided by Morten Hald, University of Tromsø, Norway. "BIOICE" samples around Iceland were collected as part of the BIOICE (Benthic Invertebrates of Icelandic Waters) project during the period 1995−1998. "MSM" samples west off Greenland were collected during the German MSM092/ cruise with RV '*Maria S. Merian*' in 2008, "POR" samples in Disko Bugt were collected during a cruise of the Danish research vessel '*Porsild*' in 1999. The type of sampling instrument is listed in the table.

Sample name	Sample no.	Sampling instrument	Water depth (m)	Latitude	Longitude
BS1191-K12+	12	Grab	224	68 °7 N	25 °54 W
BS1191-K14-1A+	14	Grab	459	68 °11 N	29 °36 W
JM96-1216/2GC+	1216	Gravity corer	478	65 °58 N	30 °38 W
JM96-1219/1	1219	Gravity corer	2144	64 °29 N	30 °27 W
JM96-1229/1GC+	1229	Gravity corer	1047	67 °1 N	25 °9 W
JM96-1234/1GC+	1234	Gravity corer	223	66 °35 N	23 °59 W
BIOICE2066	2066	Shipek grab	199	66 °9 N	17 °35 W
BIOICE2084	2084	Shipek grab	743	67 °16 N	17 °25 W
BIOICE2130	2130	Shipek grab	642	66 °47 N	18 °42 W
BIOICE2194	2194	Shipek grab	125	66 °17 N	18 °49 W
BIOICE2196	2196	Shipek grab	38	64 °18 N	22 °24 W
BIOICE2205	2205	Shipek grab	86	64 °3 N	22 °60 W
BIOICE2208	2208	Shipek grab	136	63 °59 N	23 °33 W

BIOICE2217	2217	Shipek grab	259	64°12' N	25°17' W
BIOICE2231	2231	Shipek grab	212	63°43' N	24°25' W
BIOICE2235	2235	Shipek grab	263	63°27' N	24°40' W
BIOICE2238	2238	Shipek grab	309	63°21' N	25°21' W
BIOICE2250	2250	Shipek grab	850	63°15' N	25°48' W
BIOICE2258	2258	Shipek grab	1197	63°16' N	26°30' W
BIOICE2746	2746	van Veen grab	800	67°46' N	20°51' W
BIOICE2748	2748	van Veen grab	973	68°2' N	20°42' W
BIOICE2752	2752	van Veen grab	1021	67°55' N	19°21' W
BIOICE2764	2764	van Veen grab	1198	68°5' N	17°30' W
BIOICE2770	2770	van Veen grab	492	68°36' N	16°57' W
BIOICE2775	2775	Box corer	1552	68°36' N	14°40' W
BIOICE2794	2794	Box corer	458	67°14' N	19°3' W
BIOICE2796	2796	Box corer	396	66°54' N	17°54' W
BIOICE2798	2798	Box corer	425	66°35' N	17°41' W
BIOICE2831	2831	Shipek grab	111	63°25' N	16°37' W
BIOICE2840	2840	Shipek grab	239	63°18' N	16°54' W
BIOICE2859	2859	RP sledge	2270	61°50' N	16°53' W
BIOICE2863	2863	RP sledge	2400	61°10' N	18°3' W
BIOICE2875	2875	Shipek grab	777	64°34' N	27°36' W
BIOICE2879	2879	Shipek grab	355	64°56' N	27°14' W
BIOICE2894	2894	Shipek grab	664	65°29' N	27°32' W
BIOICE2919	2919	Shipek grab	1268	65°26' N	29°11' W
BIOICE2938	2938	Shipek grab	151	65°31' N	26°13' W
BIOICE2949	2949	Shipek grab	160	65°42' N	25°17' W
BIOICE2960	2960	Shipek grab	53	65°21' N	24°5' W
BIOICE2964	2964	Shipek grab	122	65°8' N	23°36' W
BIOICE2971	2971	Shipek grab	91	65°3' N	24°13' W
BIOICE2975	2975	Shipek grab	163	65°2' N	25°52' W
MSM09/2-415	415	Box Corer	302	52°40' N	51°58' W
MSM09/2-419	419	Box Corer	2241	52°58' N	51°18' W
MSM09/2-424	424	Multi Corer	3369	53°23' N	50°15' W
MSM09/2-432	432	Box Corer	3842	54°17' N	48°0' W
MSM09/2-439	439	Box Corer	3474	56°53' N	52°41' W
MSM09/2-450	450	Box Corer	3004	60°0' N	49°0' W
MSM09/2-453	453	Box Corer	2632	62°33' N	52°38' W
MSM09/2-454	454	Box Corer	735	64°58' N	56°26' W
MSM09/2-455	455	Multi Corer	1339	68°58' N	59°34' W
MSM09/2-456	456	Multi Corer	1215	72°30' N	61°57' W
MSM09/2-463	463	Box Corer	798	71°26' N	70°26' W
MSM09/2-465	465	Box Corer	865	68°50' N	66°16' W
MSM09/2-467	467	Multi Corer	1550	68°32' N	63°20' W

MSM09/2-468	468	Box Corer	393	65°60' N	60°30' W
MSM09/2-469	469	Multi Corer	466	64°60' N	59°0' W
MSM09/2-470	470	Box Corer	1009	64°0' N	57°60' W
MSM09/2-472	472	Multi Corer	2330	62°33' N	56°28' W
POR01	1001	van Veen grab	376	69°17' N	53°5' W
POR02	1002	van Veen grab	391	69°19' N	52°51' W
POR03	1003	van Veen grab	350	68°46' N	51°33' W
POR09	1009	van Veen grab	350	68°46' N	51°23' W
POR12	1012	van Veen grab	132	69°43' N	51°48' W
POR14	1014	van Veen grab	368	69°48' N	51°51' W
POR15	1015	van Veen grab	279	69°47' N	51°50' W
POR17	1017	van Veen grab	36	69°46' N	50°54' W
POR18	1018	van Veen grab	379	69°11' N	51°49' W
POR19	1019	van Veen grab	382	69°10' N	51°27' W
POR20	1020	van Veen grab	279	69°10' N	51°18' W
POR22	1022	van Veen grab	330	68°59' N	51°38' W
POR23	1023	van Veen grab	279	69°13' N	51°10' W

3. Diatom-based transfer function for sea-ice concentration

Quantitative reconstructions of palaeoenvironments based on fossil diatom data require access to modern datasets with diatom species similar to those found in fossil datasets. In the present study, surface sediment diatom data from 72 surface samples were used to quantify the relationship between diatom assemblages and modern environmental variables (Table S2).

Detrended correspondence analysis (DCA), detrending by segments, non-linear rescaling of axes and down-weighting of rare species was undertaken on the modern diatom data in order to determine which method was the most appropriate with the gradient length (range of variation) as the criterion (ter Braak, 1988). Since the length of gradient in DCA exceeded 3 SD (3.105 and 3.838), canonical correspondence analysis (CCA) was employed to identify statistically significant relationships between the diatom assemblages and the environmental variables (ter Braak and Šmilauer, 2002; Lepš and Šmilauer, 2003). Eight environmental variables (January, February, March, May, June, July, September and December SICs) are assumed to be correlated with the others because their variance inflation factor (VIF) is greater than 20 (ter Braak, 1986), and these variables capture little variance in the diatom dataset. Only the remaining four variables (April, August, October and November SICs) have a unique influence on the diatom distribution and therefore were included for further analysis (Sha et al., 2014). Forward selection of the environmental variables and associated Monte Carlo permutation tests (999 permutations) were used to determine if each of the remaining four variables showed a statistically significant correlation to the diatom dataset. The results reveal that only April and August SICs explain a statistically significant ($p \leq 0.001$) amount of variation in the diatom data, representing 52% of the total canonical variance. The April SIC alone accounts for most of the variance (April, 38%; August, 14%), suggesting that this is the most important environmental factor controlling the distribution of diatoms, and it is therefore an important climatic variable that potentially may be reconstructed back in time beyond the period of instrumental data (Sha et al., 2014).

The computer program C2 (Juggins, 2007) was used to construct a diatom-based transfer function for reconstruction of SIC. Seven numerical reconstruction methods were tested based on the marine sediment cores: simple weighted averaging regression and calibration (WA), weighted averaging with tolerance down-weighting ($WA_{(tol)}$), each with classical and inverse deshrinking (Birks et al., 1990), partial least squares (PLS), weighted averaging with partial least squares regression (WA-PLS) (ter Braak and Juggins, 1993) and the modern analogue technique (MAT). Leave-one-out cross-validation (jack-knifing) (Birks, 1998) was applied to all models. Our results show that the WA-PLS using 3 components has the lowest $RMSEP_{(Jack)}$ (1.065) and the highest R^2_{Jack} (0.916) for April SIC (Table S3), and hence the WA-PLS using 3 components should be employed to obtain the most reliable diatom-based SIC transfer function in the area.

The performance of the final model is illustrated in the plots of modern observed values against predicted values (using a cross-validated model) based on the diatom data from the same surface samples sites, which exhibit a good linear relationship (see Fig. S3). Furthermore, the prediction error for each fossil sample, which combines the standard error of estimates for each samples with the error in the calibration function, was calculated using the software program C2 (Juggins, 2003, 2007).

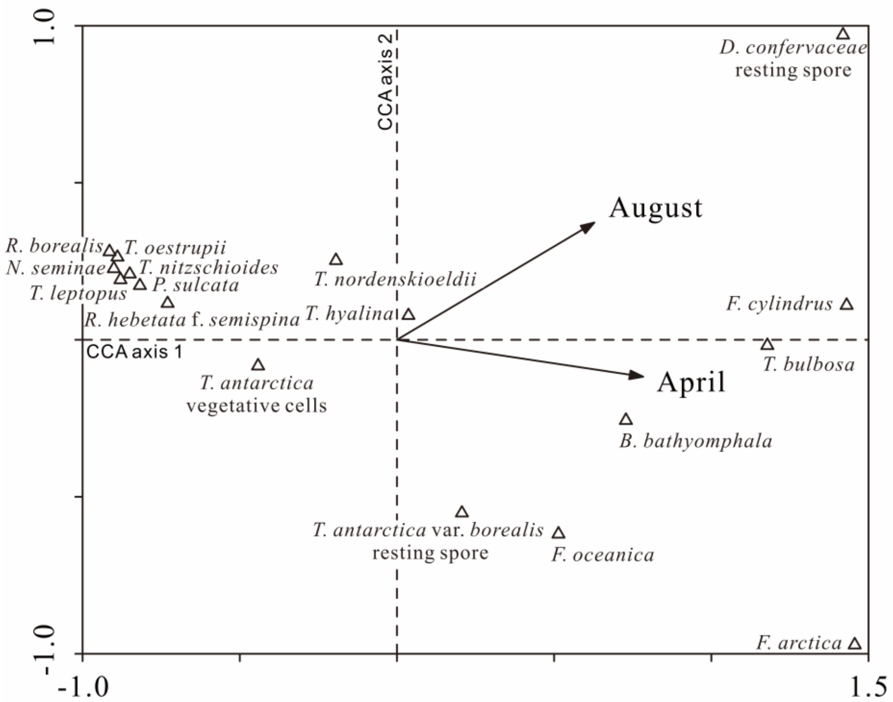

Figure S2. Canonical correspondence analysis (CCA) biplot of surface sample diatom species and environmental variables with grouping of diatom species. Modified from Sha et al. (2014).

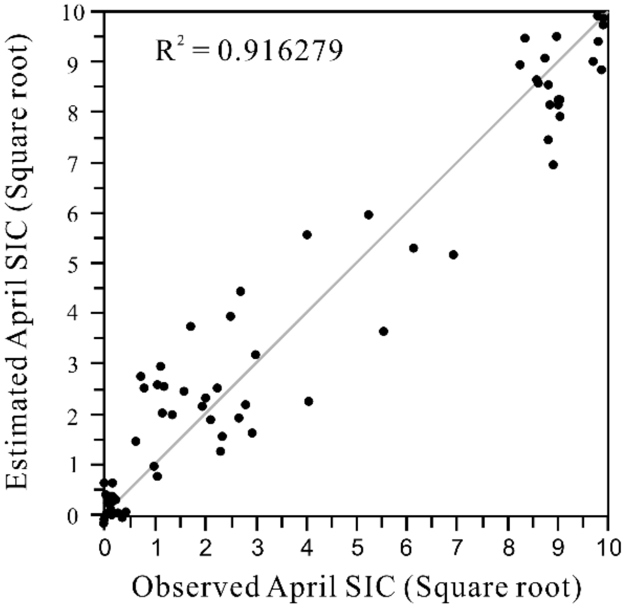

Figure S3. Plot of observed versus predicted values for the transfer function model derived for sea-ice concentrations. The SIC percentages were transformed to a square-root scale. Modified from Sha et al. (2014).

Table S3. Results of statistical evaluation of the transfer function. Maximum bias (Max $Bias_{(Jack)}$), coefficient of determination between observed and predicted values R^2_{Jack}, and root-mean squared error of prediction, based on the leave-one-out jack-knifing ($RMSEP_{(Jack)}$) for the reconstructed April SIC in seven reconstruction procedures. Both inverse and classical deshrinking regression were used in WA and $WA_{(tol)}$ reconstruction procedures. The tests indicate that WA-PLS with 3 components is the most reliable (values in bold). Modified from Sha et al. (2014).

		Max $Bias_{(Jack)}$	**R^2_{Jack}**	**$RMSEP_{(Jack)}$**
WA	Inverse	1.063	0.837	1.481
$WA_{(tol)}$	Inverse	2.956	0.818	1.585
WA	Classical	0.652	0.839	1.563
$WA_{(tol)}$	Classical	2.935	0.820	1.716
PLS	1 component	1.590	0.799	1.647
PLS	2 components	2.099	0.891	1.210
PLS	3 components	2.300	0.901	1.152
PLS	4 components	2.032	0.906	1.124
PLS	5 components	1.970	0.907	1.122
WA-PLS	1 component	1.118	0.838	1.479
WA-PLS	2 components	2.378	0.915	1.071
WA-PLS	3 components	**1.813**	**0.916**	**1.065**
WA-PLS	4 components	1.809	0.906	1.137
WA-PLS	5 components	2.173	0.894	1.212
MAT	1 analogues	2.839	0.850	1.459
MAT	2 analogues	3.321	0.876	1.309
MAT	3 analogues	3.191	0.911	1.104

MAT	4 analogues	3.457	0.909	1.113
MAT	5 analogues	2.212	0.903	1.151

4. Testing the reliability of the diatom-based SIC reconstruction

In order to further test the reliability of our diatom-based SIC reconstruction, we compared the reconstructed SIC of the last ~75 year from box core GA306-BC4, from the same location as gravity core GA306-GC4, with the satellite SIC record obtained from Nimbus-7 SMMR and DMSP SSM/I-SSMIS Passive Microwave Data (GSFC product, NSIDC-0051) for the period AD 1979-2006. We also compared our reconstructed SIC with the model SIC from the HadISST 1.1 dataset (Rayner et al., 2003), during the time interval AD 1953-2006, as well as with the mean water temperature in the upper 200 m west of Fylla Bank (section 4) for AD 1963-2006.

The diatom-based reconstructed SIC exhibits a generally similar distribution pattern to the satellite and model SIC data, as well as to the instrumental temperature records, although there are a few differences in timing of the high-resolution time series (Fig. S4). In a cross-correlation analysis between reconstructed SIC record and the satellite SIC data, the highest correlation is achieved when using a 7-year time lag (r=0.43; Fig. S5), or a 5-year time lag for detrended data (r=0.39; not shown). In fact, a plot of reconstructed SIC with a 3-year time lag already shows a similar distribution pattern as the satellite record. This may partly be caused by uncertainties in the chronology and the low temporal resolution of the sediment core. Thus, the comparison suggests that, within limits of the temporal resolution, our reconstructed SIC record based on diatom data is reliable for studies of palaeoceanographic changes off West Greenland during pre-instrumental times (Sha et al., 2014).

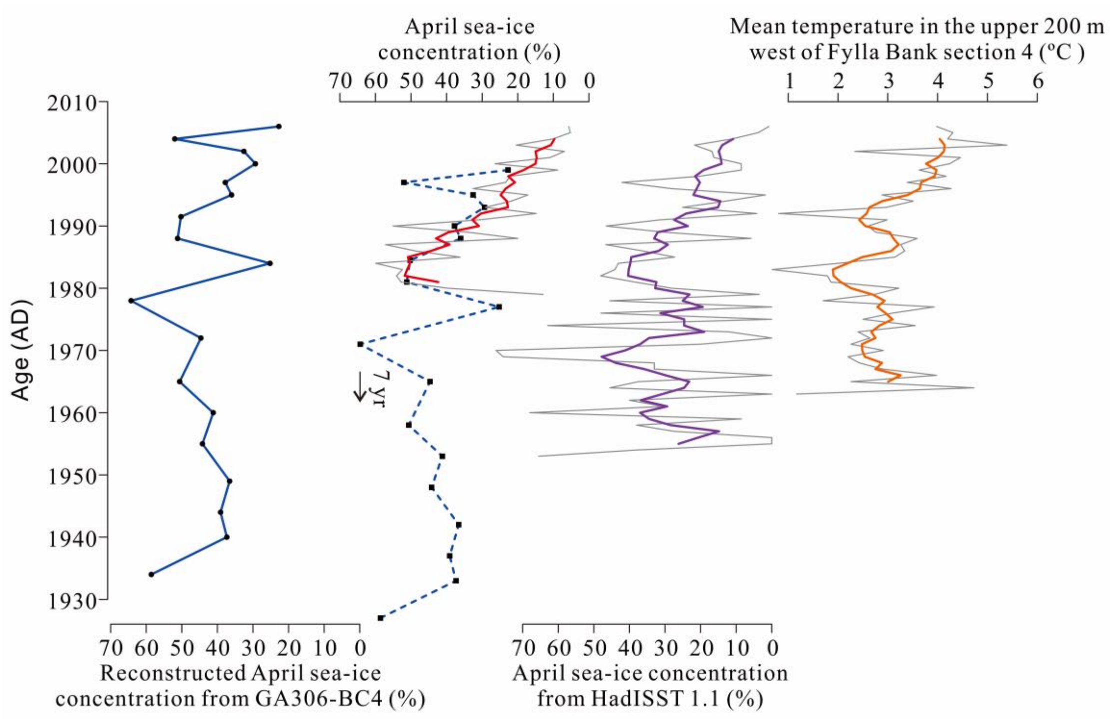

Figure S4. Diatom-based reconstructed sea-ice concentration (blue) for the period AD 1935−2006 from box core GA306-BC4 compared with the satellite April sea-ice concentration (red) from Nimbus-7 SMMR and DMSP SSM/I-SSMIS Passive Microwave Data (GSFC product, NSIDC-0051) for the period AD 1979−2006 and the model April sea-ice concentration (purple) from the HasISST 1.1 dataset (AD 1953−2006), as well as with the mean water temperature in the upper 200 m (orange) west of Fylla Bank (section 4) for AD 1963−2006. Reconstructed sea-ice concentration, adjusted by -7 years, is denoted by the blue dashed line. Actual data are shown as grey lines; smoothed records (5-point running average) are denoted by bold lines in colour. It should be noted that in contrast to the present paper, a 7-point weighted moving average method was applied by Sha et al. (2014), including previous years not centred around the actual sample. We believe this present calculation to be preferable. It should also be noted that due to age-model constraints of the sediment core record, a one-to-one correlation between reconstructed and satellite sea ice should not be expected, only the trends should be considered. The second sample from the top in the reconstructed sea-ice record is presumably an outlier.

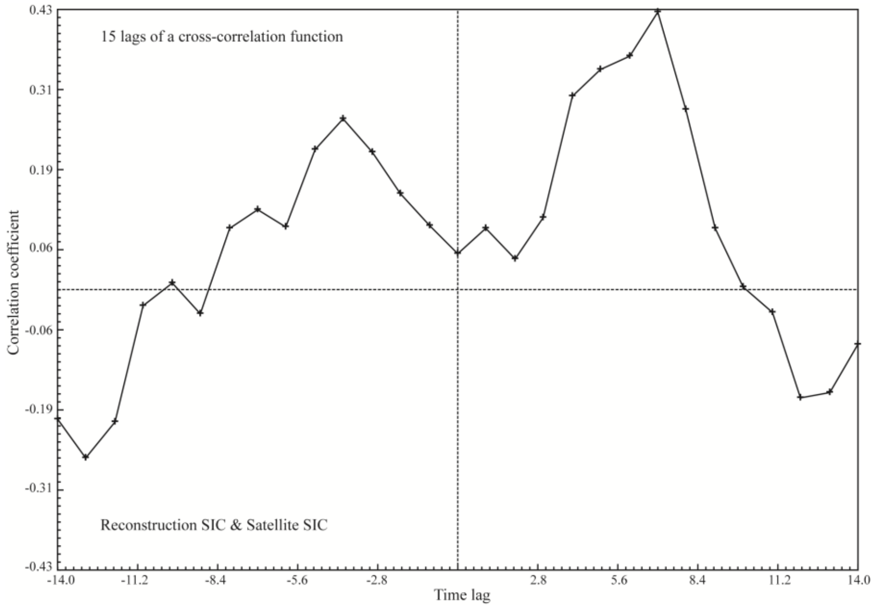

Figure S5. Cross-correlation analysis between reconstructed SIC record from box core GA306-BC4 and the satellite April sea-ice concentration from Nimbus-7 SMMR and DMSP SSM/I-SSMIS Passive Microwave Data (GSFC product, NSIDC-0051) for the period AD 1979−2006. The analysis was performed using the Crospec v. 1.4 program by Howell (2006) in the Arand package. Both records are interpolated to annual data, and subtract the mean values. This analysis shows that the maximum correlation (r=0.43) is obtained for a 7-year time lag of the reconstructed SIC record compared to the satellite record.

5. Cross-correlation analysis

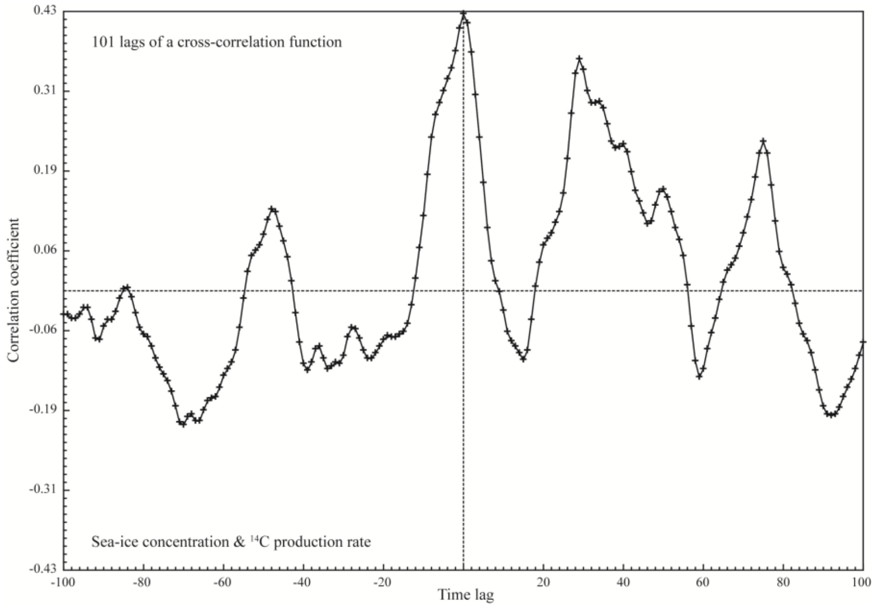

Figure S6. Cross-correlation analysis between the reconstructed SIC record from core GA306-GC4 and the ^{14}C production rate. Both records were interpolated to a common time scale with a time step of 5 years, and the mean was subtracted from each series. The analysis shows that the maximum correlation is obtained for zero lag, which means that the two records are in phase on this time scale.

6. Reconstructed sea-ice concentrations off West Greenland

Table S4. Reconstructed SIC record from gravity core GA306-GC4 off West Greenland.

Age (AD)	April sea-ice concentration (%)
1938	34.08
1927	29.42
1908	45.73
1898	44.22
1889	37.51
1879	19.90
1870	44.33
1860	41.83
1850	32.88
1840	35.36
1830	43.07
1821	48.77
1811	40.96
1802	35.05
1792	41.00
1782	40.11
1773	37.61
1763	35.22
1753	40.04
1744	29.08
1734	39.70
1724	32.91
1715	49.03
1705	47.20
1695	42.75
1686	40.09
1676	49.80
1667	60.21
1656	51.08
1646	36.38
1636	44.85
1625	38.55
1615	38.55
1605	30.32
1595	48.47
1584	42.15
1574	39.51
1564	36.55

1554	42.43
1544	37.90
1533	41.67
1523	31.55
1513	32.59
1503	47.42
1492	42.37
1482	42.06
1472	44.16
1462	37.10
1451	38.32
1441	37.29
1430	48.91
1420	37.48
1409	40.35
1388	38.65
1378	46.01
1368	33.58
1357	29.33
1347	38.68
1337	31.44
1327	44.73
1316	30.67
1306	41.08
1296	41.33
1286	38.07
1275	35.58
1265	39.59
1255	31.67
1244	35.49
1234	37.30
1223	45.32
1212	31.93
1201	41.39
1190	37.12
1179	36.97
1168	32.53
1158	44.13
1147	35.13
1137	34.17
1126	27.81
1116	39.52

1105	29.62
1095	41.80
1084	37.65
1074	36.39
1063	32.27
1053	44.27
1043	38.84
1033	42.43
1023	41.16
1012	27.49
1002	33.25
992	39.94
982	37.57
972	34.88
962	29.58
951	37.22
941	41.14
931	30.51
921	28.23

Table S5. Reconstructed SIC record from box core GA306-BC4 off West Greenland.

Age (AD)	April sea-ice concentration (%)
2006	22.74
2004	52.00
2002	32.57
2000	29.34
1997	37.80
1995	36.04
1991.5	50.25
1988	51.20
1984	25.22
1978	64.28
1972	44.65
1965	50.63
1960	41.19
1955	44.21
1949	36.59
1944	39.12
1940	37.35
1934	58.59

Supplementary References

Appleby, P.G., 2001. Chronostratigraphic techniques in recent sediments, In: Last, W.M., Smol, J.P. (Eds.), Tracking environmental change using lake sediments. Kluwer Academic Publishers, Netherlands, p. 171－203.

Birks, H.J.B., 1998. Numerical tools in palaeolimnology - Progress, potentialities, and problems. Journal of Paleolimnology 20, 307-332.

Birks, H.J.B., Line, J.M., Juggins, S., Stevenson, A.C., ter Braak, C.J.F., 1990. Diatoms and pH Reconstruction. Philosophical Transactions of the Royal Society B: Biological Sciences 327, 263-278.

Erbs-Hansen, D.R., Knudsen, K.L., Olsen, J., Lykke-Andersen, H., Underbjerg, J.A., Sha, L., 2013. Paleoceanographical development off Sisimiut, West Greenland, during the mid- and late Holocene: A multiproxy study. Marine Micropaleontology 102, 79-97.

Howell, P., Pisias, N., Ballance, J., Baughman, J., Ochs, L., 2006. ARAND Time-Series Analysis Software, Brown University, Providence RI.

Juggins, S., 2003. C2 Version 1.3 User guide. Software for ecological and palaeoecological data analysis and visualisation. Newcastle University, Newcastle upon Tyne, UK.

Juggins, S., 2007. C2 Version 1.5 User guide. Software for ecological and palaeoecological data analysis and visualisation. Newcastle University, Newcastle upon Tyne, UK.

Lepš, J., Šmilauer, P., 2003. Multivariate analysis of ecological data using CANOCO. Cambridge University Press, New York.

Ramsey, C.B., 2009. Bayesian analysis of radiocarbon dates. Radiocarbon 51, 337-360.

Rayner, N.A., Parker, D.E., Horton, E.B., Folland, C.K., Alexander, L.V., Rowell, D.P., Kent, E.C., Kaplan, A., 2003. Global analyses of sea surface temperature, sea ice, and night marine air temperature since the late nineteenth century. Journal of Geophysical Research 108, 4407.

Reimer, P.J., Baillie, M.G.L., Bard, E., Bayliss, A., Beck, J.W., Blackwell, P.G., Ramsey, C.B., Buck, C.E., Burr, G.S., EDWARDS, R.L., Friedrich, M., Grootes, P.M., Guilderson, T.P., Hajdas, I., Heaton, T.J., Hogg, A.G., Hughen, K.A., Kaiser, K.F., Kromer, B., McCormac, F.G., Manning, S.W., Reimer, R.W., Richards, D.A., Southon, J.R., Talamo, S., Turney, C.S.M., van der Plicht, J., Weyhenmeyer, C.E., 2009. IntCal09 and Marine09 radiocarbon age calibration curves, 0-50,000 years cal BP. Radiocarbon 51, 1111-1150.

Schulz, M., Stattegger, K., 1997. Spectrum: spectral analysis of unevenly spaced paleoclimatic time series. Computers & Geosciences 23, 929-945.

Sha, L., Jiang, H., Knudsen, K.L., 2012. Diatom evidence of climatic change in Holsteinsborg Dyb, west of Greenland, during the last 1200 years. The Holocene 22, 347-358.

Sha, L., Jiang, H., Seidenkrantz, M.-S., Knudsen, K.L., Olsen, J., Kuijpers, A., Liu, Y., 2014. A diatom-based sea-ice reconstruction for the Vaigat Strait (Disko Bugt, West Greenland) over the last 5000 yr. Palaeogeography, Palaeoclimatology, Palaeoecology 403, 66-79.

ter Braak, C.J.F., 1986. Canonical correspondence analysis: a new eigenvector technique for multivariate direct gradient analysis. Ecology 67, 1167-1179.

ter Braak, C.J.F., 1988. CANOCO — a FORTRAN program for canonical community ordination by [partial][detrended][canonical] correspondence analysis, principal components analysis and redundancy analysis (version 2.1), Report LWA-88-02. Agricultural Mathematics Group, Wageningen, pp. 1-95.

ter Braak, C.J.F., Juggins, S., 1993. Weighted averaging partial least squares regression (WA-PLS): an improved method for reconstructing environmental variables from species assemblages. Hydrobiologia 269-270, 485-502.

ter Braak, C.J.F., Šmilauer, P., 2002. CANOCO reference manual and CanoDraw for windows user's guide: software for canonical community ordination (version 4.5). Microcomputer Power, Ithaca (NY).